Phase transformations in PuGa 1 at.% alloy: New valuable insight into the isothermal martensitic $\delta \rightarrow \alpha$' transformation

F. Lalire, B. Ravat, B. Oudot, B. Appolaire, A. Perron, E. Aeby-Gautier, F. Delaunay

Phase transformations in PuGa 1 at.% alloy: New valuable insight into the isothermal martensitic $\delta \rightarrow \alpha'$ transformation

F. Lalire [a, c], B. Ravat [a, *], B. Oudot [a], B. Appolaire [b], A. Perron [a], E. Aeby-Gautier [c], F. Delaunay [a]

[a] CEA Centre de Valduc, 21120 Is Sur Tille, France
[b] LEM, CNRS/ONERA, BP 72, 92322 Chatillon Cedex, France
[c] Institut Jean Lamour, UMR CNRS-Université de Lorraine 7198, Parc de Saurupt, 54042 Nancy Cedex, France

This paper deals with the results of an investigation of low-temperature martensitic transformation in a metastable PuGa 1 at.% alloy. The kinetics of this process were studied experimentally via *in situ* XRD characterizations performed during isothermal holds. This revealed a double-C Time–Temperature–Transformation diagram similar to that reported in the literature for enriched alloys. The originality of our results lies in the demonstration of the existence of different martensite morphologies corresponding to the upper and lower parts of the TTT diagram. These microstructural variations seem to be the result of different accommodation mechanisms.

The experimental nucleation rate study has suggested an autocatalytic character of the isothermal martensitic nucleation process as well as a large sensitivity to elastic and plastic strain. Indeed, the incubation period and subsequent increase in nucleation rate could be related to the appearance of new embryos rather than the growth of existing plates, while the partial character of the transformation may be attributed to interactions between plates that are being formed in the two-phase $\delta + \alpha'$ alloy. These hypotheses have been confirmed by the classical heterogeneous nucleation approach by Pati and Cohen, which takes into account the autocatalytic character of the transformation. This approach has also indirectly revealed the existence of restraining forces that reflect a high sensitivity of the energy barrier for nucleation to the α' phase amount.

1. Introduction

Plutonium, which was discovered in 1942, displays highly unusual behavior that makes it the most complex element in the periodic table. As a consequence, many studies are still being devoted to the behavior of pure plutonium today [1–5]. Indeed, plutonium metal has six allotropic phases between room temperature and its melting point at ambient pressure. For Pu alloys, the existence domains of these phases are particularly sensitive to temperature, time, stress and alloy chemical composition. At room temperature, the stable phase is the brittle (simple monoclinic) α phase. The high-temperature (face-centered cubic) δ phase, which is stable from 315 to 457 °C, can also be held at room temperature and pressure by alloying plutonium with "δ-phase stabilizing" elements such as Al, Am, Ce and Ga. In PuGa alloys with Ga contents below 3 at.%, a partial transformation of δ into the martensitic α' phase involving a large volume contraction of almost 20% can be observed at subzero temperatures. The crystallographic structure of the α' phase is similar to that of the α phase of pure plutonium. In fact, there is only a small difference in lattice parameter, due to a slight expansion of the unit cell from Ga atoms being trapped in the α' lattice [6].

Martensitic transformation is a phase-change process with two main features [7]: i) it is a displacive reaction that is dominated by the strain energy arising from shear-like displacements, and entails a cooperative movement of atoms in some lattice regions; ii) it is diffusionless: the product phase inherits the chemical composition, atomic order and lattice defects of the parent phase.

There are many complex aspects in the martensitic transformation of PuGa alloys, as summarized below.

It has been shown that the martensitic microstructure of PuGa

* Corresponding author.
E-mail address: brice.ravat@cea.fr (B. Ravat).

alloys is influenced by the Ga content and consequently by the temperature of transformation. For example, Moore et al. [8] observed a twinned microstructure comprising sets of thin parallel plates in a PuGa 2 at.% alloy for a quenching at −120 °C, while Goldberg et al. [9] observed a feather-like morphology in PuGa 1 at.% during a cooling down to −25 °C.

The crystallographic aspects of martensitic transformation have also been investigated. Adler et al. [10] and Jin et al. [11] describe the process as a combination of homogeneous strain and the shuffling of alternating close-packed $(111)_\delta$ planes. Their results show that the formation of stable twins with combined variant pairs leads to an Invariant Plane Strain (IPS) solution, thereby minimizing the transformation strain energy. On a finer scale, Hirth et al. [12] analyzed the transformation in terms of a defect-based topological model, which revealed the contribution of disconnections and terrace planes.

As for the kinetics of the martensitic transformation, all experiments performed on plutonium alloys thus far indicate that the process takes place isothermally [13,14]. This isothermal character implies that both temperature and time have an impact on the extent of the transformation. Various experimental investigations conducted on PuGa alloys have revealed a Time−Temperature−Transformation (TTT) diagram that takes the form of a "double-C" curve as recently observed by Oudot et al. [15]. Many hypotheses have been put forward, but to date, the mechanisms behind these unusual kinetics have not been elucidated. Deloffre et al. [16] have suggested that this unique shape may be linked to the emergence of an intermediate γ' phase during martensitic transformation in the upper C-curve. More recently, Moore et al. [8] suggested a possible influence of the crystallographic orientation, and more specifically the existence of two different habit planes corresponding to the upper and lower C-curves. Meanwhile, based on DFT calculations, Sadigh and Wolfer propose that the existence of this double-C curve could be related to the position of gallium atoms in the monoclinic structure [17]. However, none of the above hypotheses have been thoroughly corroborated, and the origins of this type of TTT diagram remain unclear.

The thermodynamic aspects of the transformation have also been widely studied. For example, Adler et al. [18] determined enthalpy and entropy changes from calorimetry measurements. Subsequently, Turchi et al. [19] developed a database for PuGa alloys to determine the Pu−Ga phase diagram via CALPHAD-based thermodynamic calculations in ThermoCalc software.

Adler et al. [18] and Turchi et al. [19] have also calculated the transformation kinetics using a phenomenological nucleation−-growth approach, based on the heterogeneous nucleation model proposed by Kaufman et al. [7]. It should be noted that Turchi et al. used Deloffre's hypothesis (formation of γ' at higher temperatures) to attempt to reproduce the double-C curve kinetics. However, their results show that this approach does not provide a good fit to experimental data. More recently, Texier et al. [20], Ravat et al. [21] and Blobaum et al. [22] used the JMAK approach, but also found that it was difficult to accurately reproduce experimental data in a satisfactory way.

Thus, a relevant phenomenological kinetics model has yet to be identified.

Despite the many investigations that have been conducted on martensitic transformation in PuGa alloys, various aspects of this process require further elucidation. Most notably, the relationships between the transformation mechanisms, kinetics and martensite morphologies are poorly understood. Thus, the present study was undertaken with the aim of improving the current knowledge of the process; this consisted in thoroughly investigating the isothermal martensitic transformation kinetics at low temperatures in a PuGa 1 at.% alloy close to the room-temperature metastability limit of the δ phase. The originality of this work lies in a quantitative *in situ* XRD characterization of the martensitic transformation (amount and types of phases, variations in cell parameter, presence of microstrains) in addition to the analysis of the microstructures evolution for different transformation conditions.

Our study was developed in two parts. First, experimental data relating to the kinetics of the transformation were obtained over a large range of times and temperatures in order to determine a precise TTT diagram. Next, an experimentally based kinetics model was used to analyse and discuss the nucleation and growth mechanisms involved. All observations are discussed in relation to the morphology of the α' phase and the stress state of the parent δ phase. This paper is the third in a series dealing with the identification and understanding of phase transformations in PuGa 1 at.% [23,24].

2. Materials and experimental methods

δ-PuGa 1 at.% samples were homogenized, micro cut, heat treated at 360 °C to anneal structural defects induced by self-irradiation [25,26] and the potential α' and γ' phase resulting from mechanical polishing (restoration of the δ phase). More details about sample characteristics and preparation are available in a previous work [23]. A further conditioning time was carried out at room temperature for at least 12 h before samples cooling down in accordance with Jeffries et al. [27,28] and Blobaum et al. [29] works. Samples were quenched from room temperature to various isothermal holding temperatures between −20 and −140 °C at a cooling rate of 60 K min^{-1} and analyzed using *In situ* X-ray diffraction (a full description of the experimental device is also given in Ref. [23]).

Different recording times—ranging from 4 to 60 min for the beginning and the end of the transformation respectively—were used in order to accurately study the kinetics of the martensitic $\delta \rightarrow \alpha'$ transformation. Three direct quenching procedures were also performed in liquid nitrogen so that the lowest temperature of −196 °C could be reached more quickly. The samples were heated back up to room temperature via oil up-quenching, which prevented retransformation upon heating. In these cases, XRD analysis were performed at room temperature after isothermal holds lasting 10, 100 and 10 000 s.

All recorded diffraction patterns were refined by the Rietveld method via the Fullprof program [30] taking into account crystallographic structures of plutonium determined by Zachariasen and Ellinger [31,32]. Diffuse background, sample displacement, scale factor, Debye−Waller factor, phase amount and cell parameters were refined. Broadening parameters related to crystallite sizes and microstrains were also analyzed as previously detailed by Platteau et al. [33].

Furthermore, metallographic observations were carried out at room temperature with an Olympus GX51® microscope. The samples were mounted in an epoxy resin, then ground and polished mechanically with abrasive SiC papers. The microstructures were revealed by electropolishing.

3. Experimental results

Numerous diffraction diagrams were recorded. An example of a typical diagram is given in Fig. 1.

Only the characteristic peaks of the δ and α' phases were identified for all these diagrams, regardless of the transformation temperature or the holding time. We thus concluded that all the

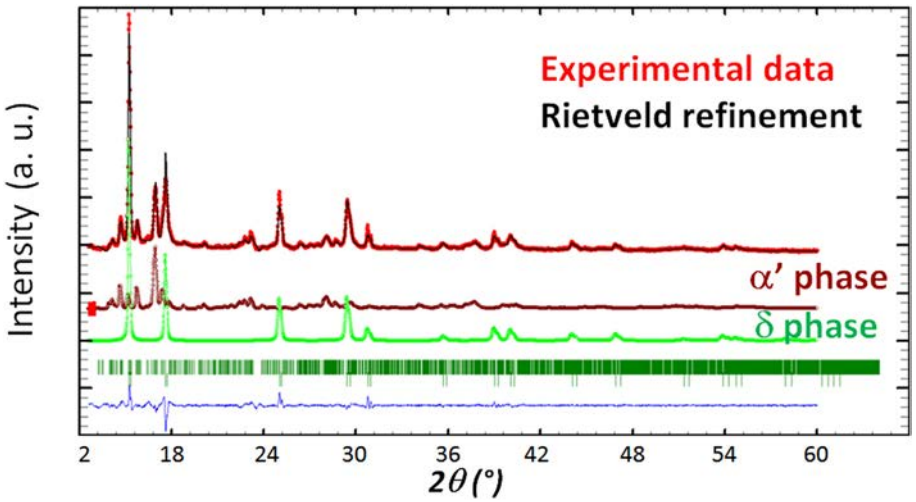

Fig. 1. Typical diffraction diagram recorded during martensitic transformation at −20 °C corresponding to a two-phase δ+α′ state in PuGa 1 at.% alloy with 40% of α′ phase and 60% of δ phase showing a good agreement between experimental data and the Rietveld refinement.

samples underwent an exclusive, direct transformation from the parent phase (δ) to the product phase (α′). As suggested in our previous paper [23], this observation disproves Deloffre's theory of an intermediate γ′ phase being the reason behind the double-C shape of the TTT diagram.

3.1. Experimental data on the kinetics of the isothermal martensitic transformation

The evolutions of α′ phase amount versus time, for the different holding temperatures, are shown Fig. 2.

The isothermal character of the transformation is clearly evidenced for the higher temperatures ranging from −20 °C to −50 °C with a clear incubation time (−20 °C to −30 °C) followed by a rapid increase in the transformation rate and a subsequent decrease. For holding temperatures lower than −50 °C, the isothermal character is still evidenced, but a large amount of transformation is formed after 4 min acquisition corresponding to the first diffraction diagram; for those temperatures, the transformation rate is continuously decreasing. The transformation may be formed either during the cooling or during the acquisition period.

From these data, the following points can be highlighted:

- Whatever the transformation temperature, a partial transformation δ→α′ is observed;
- The maximum of α′ phase amount is increasing with the decrease in temperature;
- The transformation is globally getting faster when transformation temperature is lower since the saturation of the transformation is reached earlier.

To plot the TTT diagram for PuGa 1 at.% (Fig. 3), iso-amounts of 10, 30, 60, 70 and 75% of α′ phase were obtained by fitting the kinetics experimental data. (Let's notice that, in this diagram, zero

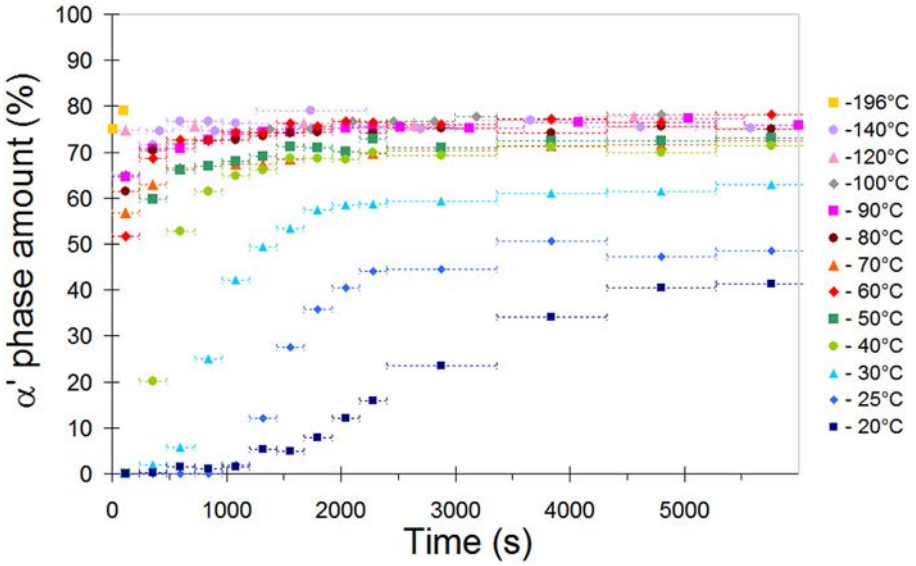

Fig. 2. α′ phase amount as a function of time for different holding temperatures highlighting the isothermal and partial character of the martensitic transformation. Generally, the transformation is getting faster when transformation temperature is lower since the saturation of the transformation is reached earlier. (An average uncertainty of 5% can be considered for the α′ phase quantification in X-ray diffraction patterns).

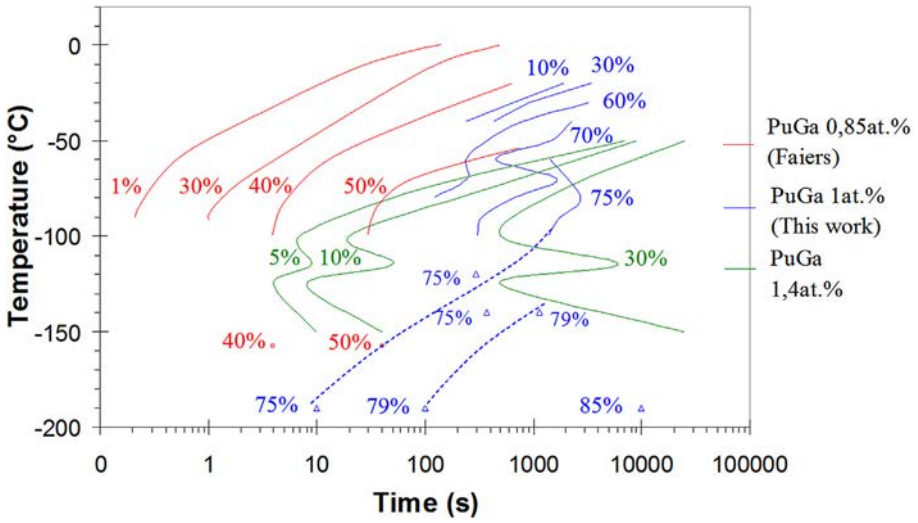

Fig. 3. Time–temperature–transformation (TTT) diagrams corresponding to the martensitic transformation of PuGa 1 at.% alloy (in blue, this work), PuGa 0.85 at.% alloy (in red, Faiers et al. [14]) and PuGa 1.4 at.% alloy (in green, Orme et al. [13]) exhibiting two distinct domains, [−20 °C; −70 °C] and [−70 °C; −196 °C]. Results are consistent with δ-stabilization by gallium addition since the iso-amounts are between those of PuGa 0.85 at.% and PuGa 1.4 at.%. An upper C-curve is evidenced by α′ iso-amounts of 60% and 70%. At lower temperature, the iso-amounts of 75% and 79% suggest rather a half of C-curve as underlined by the dashed line used as eye guide. (For interpretation of the references to colour in this figure legend, the reader is referred to the web version of this article.)

time corresponds to the time at which the transformation temperature was reached.) From these α′ iso-amounts, two distinct domains, [−20 °C; −70 °C] and [−70 °C; −196 °C], were identified. In the higher domain of temperature, the martensite iso-amounts of 60 and 70% exhibit a maximum of transformation rate at a temperature of −60 °C revealing the presence of a nose in an upper C-curve. The shape of the TTT diagram shows also that −70 °C is a limit of this upper C-curve. For the lower temperature range, it appears that the transformation duration to obtain large amounts of martensite (e.g. 75% and 79%) decreases significantly with decreasing temperature.

Our results are overall consistent with those obtained by Faiers et al. [14] for a PuGa 0.85 at.% alloy and those of Orme et al. [13] for a PuGa 1.4 at.% alloy.

Indeed, our results are in agreement with δ-stabilization by gallium addition: for transformation temperatures between −20 and −50 °C, the iso-amounts are between those of PuGa 0.85 at.% and PuGa 1.4 at.%. For lower temperatures, the transformation kinetics are faster than those of PuGa 1.4 at.%. Moreover, the gallium content seems to have an influence on the shape of the TTT diagram. For PuGa 1.4 at.% two noses of the TTT diagram are clearly evidenced, while an increase in the transformation rate is only observed down to −70 °C for our results on PuGa 1 at.%. As for the PuGa 0.85 at.% alloy, no double-C shape has been observed. Instead, it takes the form of a classical (single) C-curve, which can be explained by a lack of experimental points (leading to an incomplete TTT diagram) or the occurrence of true single-C curve kinetics. In the latter case, the kinetics of PuGa 1 at.% would lie somewhere between those of PuGa 1.4 at.% and PuGa 0.85 at.%.

3.2. Lattice parameters of the δ phase

A study of changes in the δ-phase lattice parameter during the transformation was also performed under all the isothermal transformation conditions. Examples of results obtained at −20, −30 and −60 °C are shown in Fig. 4.

The δ-phase lattice parameter was initially constant for α′ amounts ≤8%, but decreased as the transformation progressed further. At larger α′ amounts, an inversion of this trend was observed as the δ-phase lattice parameter increased sharply. It can be mentioned that this increase is correlated with the significant decrease in the transformation rate observed at large α′ phase amount, before the saturation of the transformation (Fig. 2).

The decrease of δ crystallites cell parameters at the beginning of the transformation (below the inflexion point) has to be considered carefully. Indeed, during transformation, the generated α′ crystallites exhibit a 20% lower volume than δ ones. Consequently, mainly tensile stresses are generated in the δ phase. As, our measures are obtained by the Bragg-Brentano XRD analyses mode. This device configuration enables specifically the characterization of crystallographic planes parallel and close to the surface. Thus, a decrease in the lattice planes spacing oriented in a parallel to the surface corresponds to an increase in uniaxial or biaxial tensile stress applied on δ phase crystallites on the surface, hence to an apparent reduction of the cell parameter. This is illustrated by the left blue boxes in Fig. 4. Thus the decrease in the cell parameter at the beginning of martensitic transformation results from the fact that the first α′ plates may form more easily near the sample surface since this free surface minimizes both interfacial δ/α′ and strain energies. When the stress tensor becomes triaxial due to an increase in martensite appearance around δ crystallites, the lattice planes spacing of the latter increases yielding to an expansion of the δ phase cell parameter as schematized by the blue boxes on the right in Fig. 4. The amplitude of the stress state is therefore directly varying with the α′ phase amount. Moreover, the amplitude of the lattice parameter variations illustrates that the lower the temperature, the higher the stress state of the δ phase lattice parameter. Indeed, while change in stress state at −20 °C tends only to compensate the initial decrease in cell parameters by a return to the initial δ lattice parameter as transformation kinetics is completed, a large increase exceeding the initial δ lattice parameter was noticed after an isothermal hold at −60 °C.

3.3. Microstrains in the δ phase

The previous results have been further analyzed with a characterization of the microstrains in the δ matrix using both isotropic and anisotropic refinements. In both cases, an increase in

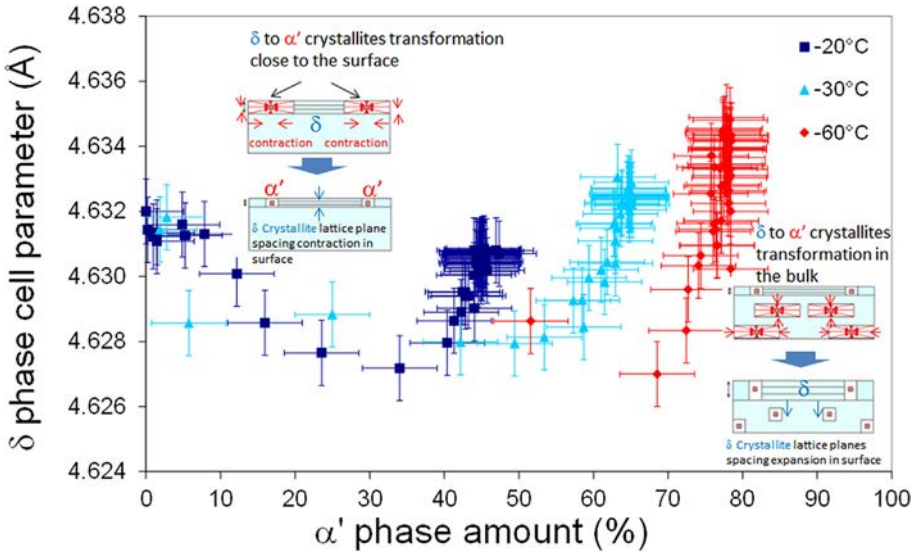

Fig. 4. Cell parameter of the δ-phase versus the α′ phase amount for isothermal transformation at −20 °C, −30 °C and −60 °C exhibiting an apparent contraction followed by an expansion of the δ phase unit cell. This behavior is related to the development of tensile stresses at the beginning of the transformation and triaxial stresses at the end as illustrated by the series of schemes (blue boxes) included in the figure and pointing out the different δ-phase lattice plane strain versus α′phase amount and their location in the sample. (For interpretation of the references to colour in this figure legend, the reader is referred to the web version of this article.)

microstrains in the δ matrix with the α′ phase amount is observed. Results are shown on Fig. 5.

The maximal value of microstrain is about 35×10^{-4} for an isotropic refinement. The large anisotropy illustrated in Fig. 5 exhibits a minimum value of 12×10^{-4} in the $[111]_\delta$ direction against a maximum value of 51×10^{-4} along $[100]_\delta$ direction.

Similar observations were previously noticed for plutonium alloyed with higher Ga content at lower temperature [33]. This large anisotropy of microstrains can be directly linked with the large anisotropy of delta phase elastic constants C_{ijkl} that exhibits the higher Zener's anisotropy factor of fcc materials (close to 6 [34]). These microstrains can thus be connected with the material stiffness in all crystallographic directions. Note that the $[111]_\delta$ direction which corresponds to a minimum of microstrains (stiff direction) is a direction normal to the closed pack plane where shuffles take place [11]. Moreover, as shown in Fig. 5, microstrains in the δ phase are α′ phase amount dependent but do not seem to be affected by the transformation temperatures.

3.4. Microstructures

The characteristic morphologies of the isothermally transformed martensite were studied with regard to the different transformation conditions.

First of all, at the macroscopic scale, we observed that the sample surface state after isothermal transformation depended on the transformation temperature. Indeed, for specimens that underwent transformation in the upper domain, large macroscopic

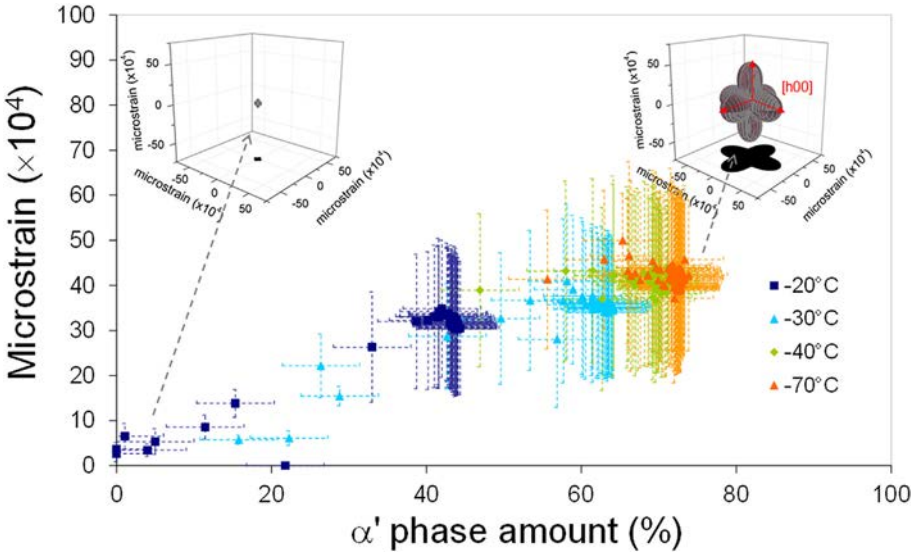

Fig. 5. Average isotropic microstrain of the δ crystallites as a function of the α′ phase amount for different holding temperatures showing an increase in microstrains in the δ matrix with the α′ phase amount. Two 3D-representations of the anisotropic microstrain corresponding to the beginning and to the end of martensitic transformation are included. This observed large anisotropy of microstrains can be directly linked with the large anisotropy of δ phase elastic constants C_{ijkl}.

plastic deformation was observed at the sample surface, as shown in Fig. 6 (specimen transformed at −20 °C).

Conversely, for specimens that underwent transformation in the lower domain, the sample surface remained completely flat, as illustrated in Fig. 8 (specimen transformed at −196 °C). Thus, significant plastic deformation occurred during transformations only in the upper temperature range.

Next, the microstructure was investigated by optical microscopy. The microstructure of the alloy observed at room temperature consisted of a single δ phase with an average grain size of 60 μm.

In the upper domain, the martensite had a feather-like morphology, which can be described as parallel plates of the α′ phase interconnected by a series of smaller, secondary α′ plates (Figs. 6 and 7).

This kind of morphology was previously observed by Goldberg et al. [9]. As Fig. 6 shows, the isothermal martensite plates were not uniformly distributed and seemed to have spread across the δ grains in a cobweb pattern, marked by narrow and continuous transformed regions. Furthermore, as shown in Fig. 7, the maximum thickness of the martensite plates after 15 000 s at −20 °C was the same as that after 1500 s at −20 °C. This indicates that the transformation progressed by the formation of new plates rather than the growth of existing plates. Further analyses revealed that the largest plate length was close to 60 μm, which could be correlated with the mean size of a δ grain. As the transformation progressed, the mean plate size decreased. Three characteristic plate sizes were identified, namely 60, 25 and 4 μm corresponding to the largest, intermediate and smallest sizes respectively.

In the presence of a volume partitioning effect, the largest plates form at the beginning of the transformation. Indeed, the initial (δ) grain size determines the size of the first plate that forms, which in most cases extends across the grain. This first plate divides the δ grain volume into two domains, in which smaller plates with different orientations form [35]. Thus, we believe that the smallest plate that we observed (4 μm) formed during the later stages of the transformation. Similar conclusions were drawn from the results at −40 °C. It should be noted that the transformation temperature seemed to have a direct influence on the number of plates rather than their size.

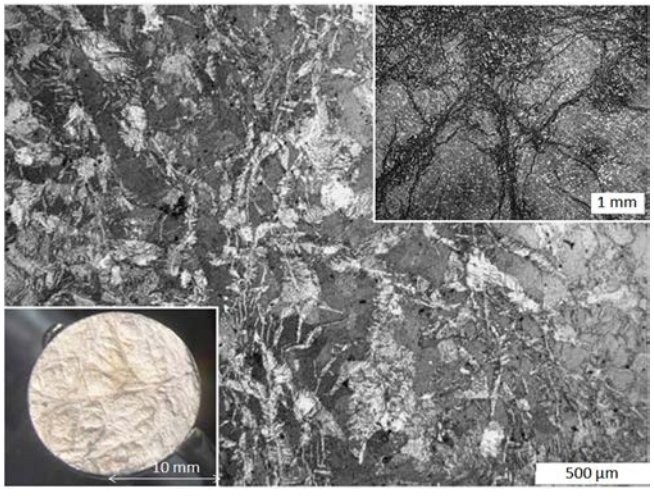

Fig. 6. Optical micrographs of PuGa 1 at.% sample transformed at −20 °C (end of the transformation) illustrating the non-uniform distribution of martensite and a feather-like morphology. Furthermore, as observed at the macroscopic scale (at the sample surface), martensitic transformation leads to large macroscopic plastic deformation at −20 °C.

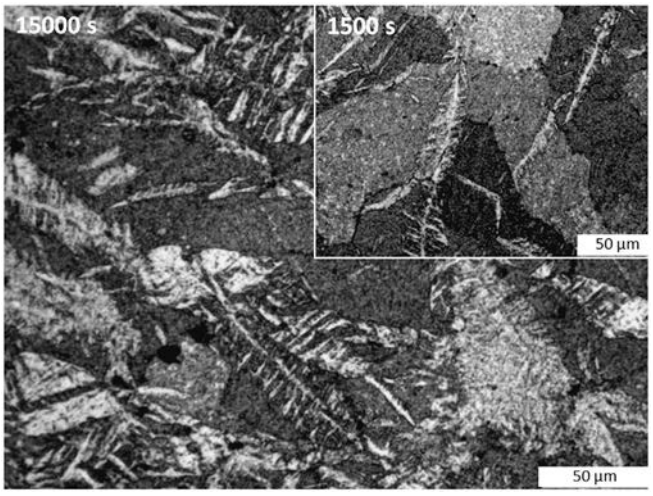

Fig. 7. Optical micrographs of PuGa 1 at.% sample maintained at −20 °C for 1500 s (5% of α′phase amount) and 15 000 s (45% of α′phase amount). Pictures exhibit the martensite feather-like morphology which can be described as parallel plates of the α′ phase interconnected by a series of smaller, secondary α′plates (the largest, intermediate and smallest sizes are 60, 25 and 4 μm). Occurrence of new feathers with reduced mean size due to the lower size of the remaining δ phase shows that transformation progresses overall by nucleation of new feathers rather than the growth of existing plates.

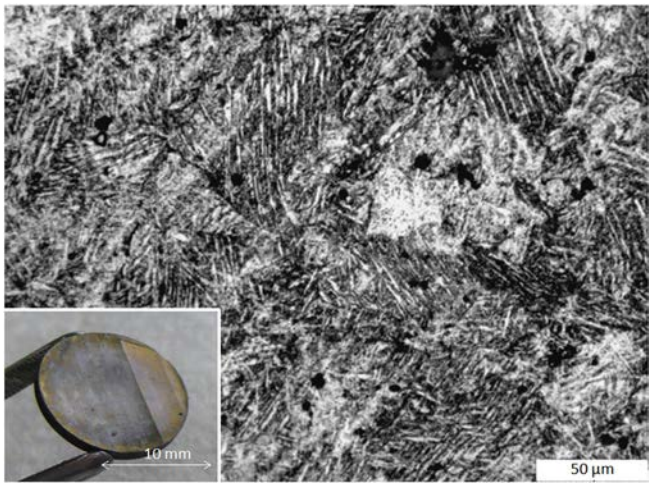

Fig. 8. Optical micrographs of a PuGa 1 at.% samples after an isothermal hold at −196 °C for 100 s (79% of α′phase amount) exhibiting martensite morphology which consists of a succession of very thin parallel plates with mean constant size. Furthermore, it appears that the sample surface remains completely flat during transformation in the lower domain.

Characteristic morphologies of the δ→α′ transformation in the lower domain of the TTT diagram were also studied on PuGa 1 at.% samples after isothermal holds at −70 °C and −196 °C. Whereas the martensite morphology at −196 °C (Fig. 8) was revealed completely different in comparison with the typical one previously detailed for the first C-Curve upper domain, the martensite morphology observed at −70 °C seemed to be a combination of the two last.

Morphology obtained at −196 °C can be regarded as a succession of very thin parallel plates with even different “variants” in a same δ grain with different variants orientations. Their mean size seems constant whereas different sizes as already observed for enriched alloys. It also appears that the thickness of the plates is

lower than that of the plates formed in the upper domain. It can be emphasized that after transformation, the size of untransformed remaining δ domains is homogeneous and much lower than for transformation at higher temperatures (upper C-curve).

4. Phenomenological analysis of transformation kinetics

To further investigate the transformation kinetics, a phenomenological analysis was performed based on the model developed by Pati and Cohen [36] describing the kinetics of isothermal martensitic transformation in non-thermo-elastic iron−−nickel−manganese alloys. This approach considers that transformation occurs by a combination of nucleation and growth processes. The nucleation is heterogeneous. Transformation occurs as a result of thermal fluctuations that are sufficient to allow the growth of embryos into martensite plates by a rapid expansion of dislocation loops surrounding the embryos [7]. In addition to the growth of existing embryos, transformation progress is linked to the formation of new embryos resulting from local stress fields surrounding the plates that are being formed (autocatalytic effect).

The Pati and Cohen model is characterized by the following equation:

$$\frac{df}{dt} = [n_i + fp - N_V](1-f)\nu exp\left(\frac{-\Delta W}{RT}\right)\left(\bar{v} + \frac{\partial \bar{v}}{\partial ln N_V}\right) \quad (1)$$

Where f is the α' phase amount, t is the time (s), n_i is the initial number of embryos per volume unit of parent phase (cm^{-3}), p is the autocatalytic factor, number of embryos generated per volume unit of martensite formed (embryos cm^{-3}), N_v is the number of martensite plates per volume unit (cm^{-3}) with $N_V = f/\overline{V}$, ν is the lattice vibration frequency (s^{-1}). ΔW is the energy barrier for martensite formation (J mol^{-1}). R is the perfect gas constant (J mol^{-1} K^{-1}). T is the isothermal hold temperature (K). $\bar{v}$ is the mean volume of observed plates (cm^3).

These factors have to be determined in order to calculate the transformation kinetics.

4.1. Parameters assessment

4.1.1. Initial number of embryos n_i and lattice vibration frequency ν

The initial number of embryos per unit volume of parent phase, n_i, was assessed from optical micrographs of the PuGa 1 at.% alloy. As mentioned above, the average diameter of the δ grains was approximately 60 μm (Fig. 8). We assumed these grains to be spherical, which led to a grain volume of 1.13×10^{-7} cm^3. The chosen value of $n_i = 10^9$ embryos cm^{-3} gave approximately 100 embryos per grain, corresponding to a distance of approximately 12 μm between embryos. This seemed to be a realistic order of magnitude and was therefore chosen for the phenomenological analyses.

In order to enable comparisons with the literature, we considered two limiting values: $n_i = 10^7$ embryos cm^{-3}, as proposed by Pati and Cohen for FeNiMn alloys [36], and $n_i = 2 \times 10^{12}$ embryos cm^{-3}, as proposed by Turchi et al. for PuGa alloys [19]. These values were tested with the aim of refining our experimental kinetics data. The influence of this parameter proved to be minimal, suggesting that the initial number of embryos may not be a predominant parameter in martensitic transformation.

Both Pati and Cohen and Turchi set the lattice vibration frequency to 10^{13} s^{-1}. This parameter may also be calculated from the results obtained by Wong based on HRIXS analyses [37]. Indeed, the author determined the phonon state density distribution as a function of energy for a δ-phase PuGa 2 at.%; this led to a mean lattice vibration frequency of 1.64×10^{12} s^{-1} for an average phonon energy of 6.8 meV. In view of these close results, we decided on a realistic value of 1×10^{13} s^{-1}.

4.1.2. Martensite plate volume

For a transformation in the upper domain of the TTT diagram, we considered that martensite plates are ellipsoidal with shape ratios of $a/b = 20$ as observed on the micrographs. The ratio a/c was supposed close to 1.5 since some δ grain areas in Fig. 7 are completely transformed supposing the observation of a slice of the feather in the $(0, \vec{a}, \vec{c})$ plane. Three mean sizes of the martensite plates were observed experimentally. The biggest plates (60 μm long) correspond to the first plates formed in the parent δ-phase. After that, intermediary plates of 25 μm length are progressively formed around the first ones. Finally, smaller plates of 4 μm length are progressively formed in the remaining volume of δ phase. In the lower domain of the TTT diagram, the morphology of martensite consisted of thin parallel plates exhibiting a length distribution from 60 μm to 20 μm. The martensite shape is still ellipsoidal, but with a ratio of $a/b = 25$ and the consideration that $b = c$.

Despite of the plate size characterization in both domains, the variation of the mean plates volume $\bar{v}$ was difficult to achieve because it was not possible to count precisely the number of plates. So, to take into account the decrease in plate size mean volume with the extent of the transformation, we have tested different volume evolutions $\overline{V}$ with the transformation amount. Finally, a linear evolution of plates mean volume was considered for the upper and lower domains. The relations used are given by the following equations:

$$\overline{V} = \left(-3.77 \times 10^{-9}\right)f + 3.77 \times 10^{-9} \quad (2)$$

$$\overline{V} = \left(-2.178 \times 10^{-12}\right)f + 1.810 \times 10^{-10} \quad (3)$$

4.2. Autocatalytic factor and energetic barrier refinement

Autocatalytic factor p and energetic barrier ΔW play a major role in the transformation kinetics and have to be determined. Both of these were obtained by means of a fit to the experimental data, which consisted in considering a single p value for all transformation temperatures and different values of ΔW for each temperature. Initially, ΔW was made to remain constant at a given temperature.

4.2.1. Reproduction of the early stages of transformation

The autocatalytic factor p is a key factor for reproducing some typical transformation characteristics such as incubation time and acceleration of transformation. Indeed, this parameter is highly sensitive to the early stages of the transformation. Therefore both autocatalytic factor p and energetic barrier ΔW were refined on the basis of the data recorded up to the inflexion point from which transformation rate decreases to match kinetics data. For instance, zoom included in Fig. 9 shows a good refinement is achieved with a p value of 9×10^{10} embryos cm^{-3} and a ΔW value of 85 400 J mol^{-1} for transformation occurring during an isothermal hold at −20 °C. Indeed the incubation time and the acceleration of the transformation are well reproduced. We can also note that our p value of 9×10^{10} embryos cm^{-3} is relatively close to this one proposed in the literature by Pati and Cohen ($p = 10^{10}$ embryos cm^{-3}). Next, this p value of 9×10^{10} embryos cm^{-3} was retained constant for the other kinetics analyses for all the isothermal hold temperatures.

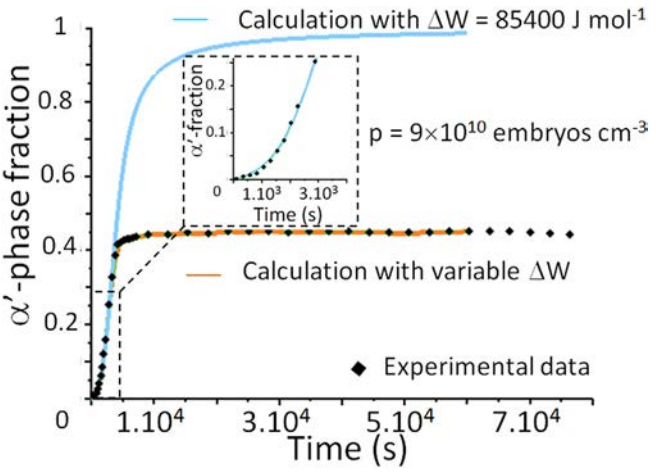

Fig. 9. Calculated curves using Pati and Cohen model compared to experimental kinetics data the isothermal hold at −20 °C. The model considers an autocatalytic factor p of 9 × 10^{10} embryos cm^{-3}. A constant ΔW value of 85 400 J mol^{-1} enables to reproduce the beginning of the transformation namely the incubation time and the acceleration of transformation (zoom). The decrease in transformation rate and its partial character could only be described by using increasing ΔW values.

4.2.2. Reproduction of the whole transformation course

With the previous refined values of p and ΔW, a gradual increase in discrepancy between both experimental and calculated amount of α′ phase is observed. Therefore, we refined the determination of ΔW even further by allowing it to vary as the transformation progressed. The experimental and calculated kinetics for both constant and variable values of ΔW are shown in Fig. 9 for a transformation temperature of −20 °C. A good fit was obtained for a variable ΔW.

The fitted values of ΔW for transformation temperatures ranging from −20 to −60 °C are shown in Fig. 10a. For all these temperatures, the ΔW variations followed a similar pattern although their absolute values were different.

At each temperature, the value of ΔW remained constant at the beginning of the transformation, then increased toward the end of the transformation. Moreover, a shift of the inflexion point of the curve towards higher α′ phase amounts was observed with decreasing temperature.

The model was also applied to the lower transformation temperatures, for which only partial experimental data on the transformation kinetics were available. A good description of the transformation kinetics was obtained with the variable values of ΔW shown in Fig. 10b. As with the higher temperature range, these ΔW values decreased with decreasing transformation temperature. They also followed a similar pattern of variation with transformation progress.

5. Discussion

Our *in situ* XRD investigation of the kinetics of martensitic transformation in PuGa 1 at.% clearly points to the isothermal character of this transformation. As no diffraction peaks characteristic of the γ′ phase were observed whatever the transformation temperature, the present results support the direct δ-to-α′ transformation process that we have previously mentioned [21]. In addition, characterization of the cell parameter variation of the parent phase clearly revealed that elastic stresses are generated in the phases as well as plastic strain at least for the higher holding temperatures. Different studies have shown that stress and plastic strains have a large influence on the martensitic transformation leading to changes in the transformation kinetics, the existence of transformation plasticity and changes in the microstructure (plate orientation and changes in plates morphology) [9]. Thus, all these factors must be considered.

In the following paragraphs, we discuss the kinetics of this isothermal phase transformation in detail, from the initial to the very last stages. We begin with nucleation sites and transformation progress. While dislocations and α/β-Pu precursors can be considered as potential sites of heterogeneous nucleation, the present study focuses on the competition between a large autocatalytic effect that promotes the transformation and interactions that act as restraining forces.

The martensite morphology strongly influenced by the transformation temperature is also discussed. The morphological variations are examined based on comparisons with martensite morphologies in steels, with emphasis being placed on the role of transformation strain accommodation processes according to the transformation temperature. All of these aspects are dealt with in detail below.

5.1. Initial stage: nature of heterogeneous-nucleation sites

Solid−solid phase transformations are generally characterized by heterogeneous nucleation, with preferential nucleation sites such as inclusions, dislocations, grain boundaries and vacancies. This is because ideal conditions like defect-free materials are particularly rare [7]. However, the nature of such sites in plutonium alloys is still widely debated: some authors cite the presence of dislocations while others highlight the existence of α and/or β

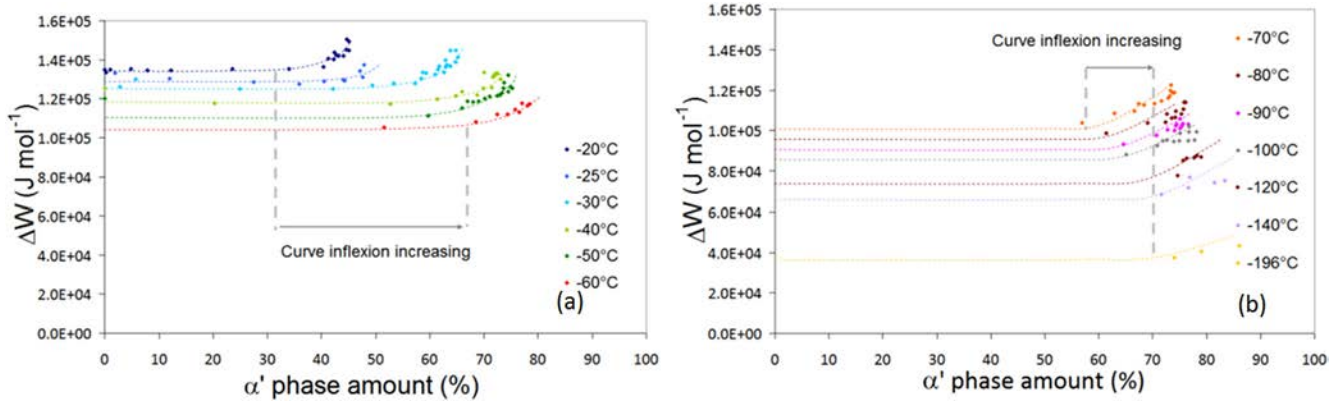

Fig. 10. Best fit of ΔW values at each step of the transformation in the upper (a) and lower (b) C-Curves enabling to reproduce the whole transformation kinetics for the different holding temperatures (with an autocatalytic factor p equal to 9 × 10^{10} embryos cm^{-3}).

precipitates/inclusions in the matrix [8,27,29].

TEM analyses performed by Moore et al. [8] on a partially transformed PuGa alloy revealed the initial presence of numerous dislocations in the sample. The authors determined the dislocation density in the δ phase in different areas. They obtained a value of 1.7×10^{11} cm^{-2} near an α′ plate, while the average background density away from the plate was 2.2×10^{10} cm^{-2}, thereby indicating the presence of initial dislocations in the δ matrix. It should be noted that the large volume contraction involved in the martensitic transformation led to local plasticity and an increase in the average dislocation density around the α′ plate by a factor of 7.7.

Blobaum et al. [29] and Jeffries et al. [27] have suggested the existence of another kind of preferential nucleation site in the δ phase, namely α and/or β precipitates/inclusions that appear during conditioning. The conditioning temperature seems to have a strong influence on the nature and amount of precipitates. Indeed, conditioning that is performed close to room temperature promotes the appearance of α nuclei, whereas conditioning at temperatures above 100 °C gives rise to β nuclei. In an attempt to eludicate the embryo structure, Platteau et al. [38] performed short-range order studies on PuAl alloys by means of a Pair Distribution Function (PDF) analysis, but no precise conclusion about the nature of inclusions could be drawn. In addition, there are as yet no direct experimental observations of nuclei that confirm the existence of such inclusions. Nonetheless, this hypothesis has not been refuted.

In summary, both dislocations and inclusions are thought to be favorable initial heterogeneous-nucleation sites for martensite formation in plutonium alloys. However, while the presence of dislocations has been clearly observed experimentally, the lack of data proving the existence of α/β-Pu inclusions in the δ matrix after a conditioning treatment has led to the hypothesis of the coexistence of different types of preferential nucleation sites.

5.2. Transformation progress

5.2.1. Phenomenon involved at the start of the transformation: autocatalytic effect

Based on our study of the isothermal transformation kinetics (Fig. 2) and the corresponding microstructures, we believe that the transformation progress is partly controlled by an autocatalytic nucleation process. Indeed, at relatively high temperatures, the transformation starts by a slow nucleation rate (incubation time), which was interpreted by Shih et al. [39] and then by Raghavan and Entwisle [35] for ferrous alloys by a very low density of favorable embryos. At the lower temperature, the incubation stage is so reduced that it could not be characterized. In a second step, whatever the transformation temperature, the transformation rate is significantly accelerated. This large acceleration of the transformation kinetics can be due to two different processes: the first one is the stimulation of additional nucleation events, notably those involved by strain/stresses surrounding the plate formed (e.g. the autocatalytic nucleation process) and the second one consists of the growth of existing plates.

The martensite feather-like morphology observed in the upper C-curve of the TTT diagram has emphasized the existence of a large autocatalytic effect since the inhomogeneous spatial distribution of transformed grain (cobweb microstructure) and more especially the lack of thickening phenomenon during the isothermal transformation are particularly characteristic of the stimulation of additional nucleation sites. Moore observations by TEM revealed the increase in dislocation density near the martensite plates in partly transformed specimen. These dislocations may lead to an increase in the density of nucleation sites as well as the existence of local stresses as revealed by the shift of the δ cell parameter, which could favour the transformation with an additional driving force associated with the transformation. Indeed, on the basis of Patel and Cohen theory [40] and Adler et al. works [41], the mechanical driving force involved by several stress states were evaluated highlighting potential energy gains depending on the martensite plate orientation in the δ matrix. While a compression state systematically induces an energy gain promoting the transformation, the effect of a tensile state, as revealed by the δ lattice parameter study (§3.2), is more complex. Indeed, uniaxial or biaxial tensile stresses existing at the beginning of the transformation can act as a driving force only on specific δ crystallites orientation.

The occurrence of a large autocatalytic nucleation process is also supported by the phenomenological formalism used. Indeed a good fit of experimental transformation kinetics could not be achieved using Kaufman and Cohen model [7], which considers a heterogeneous nucleation process with a constant number of embryos all along the transformation. The introduction of an autocatalytic phenomenon was necessary and sufficient to reach a good description of the incubation period and the large acceleration of the transformation kinetics.

All of these observations emphasize the major role of the autocatalytic effect during isothermal martensitic transformation in PuGa 1 at.% alloys. However, it cannot be the only factor controlling the transformation progress. Indeed, while it easily accounts for the plate distribution and the first part of the kinetics involving a large acceleration of the nucleation rate, it is in direct contrast with the partial nature of the transformation as well as the decrease in transformation rate.

5.2.2. Decrease in transformation rate: occurrence of interactions

Our results show a decrease in the transformation rate as the transformation progresses. They also indicate that the maximum amount of martensite obtained when the transformation reaches saturation increases with decreasing holding temperature. These observations suggest the occurrence of unfavourable interactions between the plates being formed and the δ + α′ mixture, which could have an impact on the transformation kinetics. Such interactions are associated with an accumulation of elastic/plastic strains in the δ phase around the α′ phase that forms. This phenomenon can be unfavourable to the process.

Indeed, we observed that for all the different transformation temperatures, a large increase in the δ-crystallite lattice parameter accompanied a decreasing transformation rate before the transformation reached saturation (Fig. 4). This clearly implies a change in the stress state as the transformation progresses and also points to the influence of the surrounding medium (mixture of δ and α′).

At larger transformation amounts beyond the inflexion point, the increase in the δ cell parameter observed for all transformation temperatures can be linked to a triaxial tensile state (tending to a hydrostatic tensile state) arising from the presence of α′ crystallites around δ crystallites. According to the Patel and Cohen theory [40], a relatively isotropic tensile stress state, whether hydrostatic or triaxial, constitutes a true restraining force that prevents the transformation. Moreover, the larger the α′ phase amount, the higher the magnitude of the stress state, which thereby reduces the driving force for martensitic transformation.

Although the Pati and Cohen phenomenological approach gave an accurate description of the beginning of the transformation with a constant transformation barrier ΔW, a discrepancy occurred from an α′ phase amount as observed from the isothermal kinetics at −20 °C (Fig. 9). This implies that even if the decrease in transformation rate can be connected with a reduction of the number of embryos potentially available for nucleation or a decrease in

martensite plate size, it would also be controlled by another influent phenomenon.

The subsequent consideration of a variable potential barrier in the Pati and Cohen model yielded a good description of the complete kinetics for all the transformation temperatures. The ΔW values that provided a good fit to the experimental data decreased with decreasing transformation temperature. At each temperature, ΔW was initially constant, then increased significantly during the rest of the transformation.

This pattern in the variation of the potential barrier during the transformation can be linked to either a decrease in the driving force associated with the local stress state or an increase in the strain energy associated with the transformation. Indeed, in the absence of any external stress state, the energy balance associated with the austenite-to-martensite transformation involves chemical bulk free energy that encourages the transformation and non-chemical energies that generally act as restraining forces, namely interfacial energy and strain energy arising from the large volume contraction associated with the transformation (20%) as well as shear components of the transformation tensor [11].

In an isothermal transformation, the chemical driving force is constant and the interfacial energy can be considered to be negligible to a first approximation. During martensitic transformation in PuGa alloys, the volume change is extremely large, and elastic and plastic strains are generated and accumulated as the transformation progresses. This has been confirmed by the final macroscopic deformation observed in our sample transformed at −20 °C (Fig. 6) as well as the higher dislocation density near martensite plates observed by Moore et al. [8]. As the amount of martensite increases, new plates form in a δ + α′ mixture of increasing mean elastic modulus. Moreover, there will be an additional resistance to the motion of dislocations due to some work hardening and to a continuous decrease in the size of δ domains. Those factors result in an increase of the deformation energy and in consequence to an increase in the restraining forces. The slowing down of the kinetics and the increase in ΔW can thus be associated with the triaxial tensile stress of δ crystallites due to the volume decrease associated with α′ crystallites formation and to an increase in the deformation energy associated with the formation of the plates.

Our results have also clearly shown that the decrease in temperature favours the transformation, which involves a gain in driving force which is in accordance with the decrease in ΔW. However, the amplitude of this decrease in ΔW cannot be only explained by the increase in chemical driving force since a negligible absolute variation of 7 J mol^{-1} K^{-1} is noticed on the temperature range of this study.

On a theoretical point of view, the decrease in temperature could generate an increase in yield strength of the δ phase, which inevitably limits the stress relaxation by plastic deformation as observed for the macrograph of specimen transformed at −196 °C (Fig. 8). Consequently, during the transformation process, the δ parent phase could exhibit higher stress levels that would lead to a higher contribution of the local stresses to the transformation progress and a decrease in ΔW as well as to limited resistance to dislocation motion during the plate growth.

All these observations indicate that it is a combination of the local stress state and the strain energy that influences the transformation progress. Transformation strains are accommodated by plastic strains to varying degrees, according to temperature. The stress state also varies with temperature and the extent of the transformation. Based on our experiments, we propose that as the transformation progresses, the stress state initially favors the transformation. Because of interactions between the new plates that form in α′ + δ, the stress state evolves into a triaxial tensile state approaching a hydrostatic tensile stress, which is not conducive to the transformation. In addition, the resistance to dislocation motion leads also to an increase in the restraining forces for the transformation.

5.3. Martensite morphologies

Our results demonstrate the existence of two different martensite morphologies for the upper and lower domains of the PuGa 1 at.% TTT diagram: a feather-like morphology at relatively high temperatures [−20 °C; −70 °C] and thin parallel plates at the lower temperatures [−70 °C; −196 °C]. This thin-plate morphology is similar to that of martensite formed at temperatures below −110 °C in alloys with higher Ga contents [8,27,28,42].

Feather-like martensite can be described as an arrangement of lenticular plates. A comparison with martensitic steels shows that the morphology corresponding to the upper C-curve of the PuGa 1 at.% TTT diagram may have a similar sort of irregular interface between the parent δ phase and the product α′ phase, in the form of a varying habit plane along each lenticular plate. The “low-temperature” morphology is comparable to that of thin-plate martensite in steels, which generally exhibits a twinned microstructure. This change in morphology is usually associated with a change in the lattice invariant strain from slip to twinning [43]. Moreover, according to recent results obtained by Miyamoto et al. [44] from an EBSD analysis of the austenite surrounding martensite plates, for thin-plate martensite the shape strain is accommodated by elastic deformation in the austenite, while for lenticular plates this accommodation involves plastic deformation in the austenite.

In the alloy that we studied, the morphological and microstructural features of the martensite proved to be particularly sensitive to temperature. Given that yield strength is highly temperature and microstructure dependent, it can easily govern the accommodation mechanism of the transformation shape strain. Consequently, the feather-like morphology occurring at relatively high temperatures may be explained by both elastic and plastic accommodation. Conversely, a decrease in temperature involving an increase in yield stress, which reduces the dislocation motion capability, implies mostly the existence of an elastic accommodation of the shape strain in the parent phase and gives rise to very thin parallel plates. The occurrence of noticeable plastic deformation when transformation happens at the higher temperatures was evidenced Fig. 6. Moreover, the feather like morphology can be compared to the morphology of stress/strain induced martensite observed by Goldberg et al. [9] in PuGa alloys. Indeed for martensite formed in those conditions, the morphology changes, tending to larger plates, the growth being favoured by the possibility to accommodate the shape strain by plastic deformation. Such changes were also reported for stress/strain induced martensite or bainite in steels [45–47]. Furthermore, the consequence of different accommodation modes during martensitic transformation versus temperature seems also to be at the origin of the different macroscopic observations. Indeed, the development of elastic and overall plastic strains at relatively high temperature is certainly responsible for the sample surface deformation (noticeable at the macroscopic scale) whereas the considered purely elastic accommodation conceivable at very low temperature explains the unchanged surface of the sample remaining flat even with a large α′ phase amount. These temperature-dependent martensite morphologies raise the question of the existence of a direct relation between variations in accommodation mechanisms and the origin of the double-C curve kinetics in the TTT diagram.

6. Conclusions

The present investigation of the kinetics of isothermal martensitic transformation in PuGa 1 at.% has revealed the direct and partial character of this transformation, regardless of the temperature or duration of the isothermal hold. The kinetics exhibit several distinct features that can be summarized as follows:

- An incubation period that may be related to the absence of favorable embryos;
- A large acceleration of the transformation rate associated with an important autocatalytic effect that controls nucleation;
- A saturation of the transformation leading to a systematic partial isothermal martensitic transformation due to the occurrence of interactions between the forming plate with the $\delta+\alpha'$ mixture which are exceeding driving forces.

These kinetics also display a certain sensitivity to the temperature of the isothermal hold. Indeed, the experimentally obtained PuGa 1 at.% TTT diagram has a double-C shape, which agrees with prior experiments performed on richer PuGa alloys. Different martensite morphologies occur for the two domains of the TTT diagram. The temperature of the isothermal hold influences the accommodation mechanisms, which may in turn account for the double-C shape of the TTT diagram. Indeed, a feather-like morphology that may be attributed to elasto-plastic accommodation occurs at relatively high temperatures (upper C-curve), whereas very thin parallel plates reflective of elastic accommodation appear at lower temperatures (lower domain).

References

[1] S.M. Ennaceur, Methodology for describing the $\alpha \rightarrow \beta$ phase transformation in plutonium, Thermochim. Acta 539 (2012) 84–91.
[2] S.M. Ennaceur, A differential scanning calorimetry study of the kinetics of the $\beta \rightarrow \gamma$ phase transformation in plutonium, Thermochim. Acta 547 (2012) 99–105.
[3] S.M. Ennaceur, The effects of thermal conditioning and recovery processes on the $\delta \rightarrow \gamma$ phase transformation mechanisms in plutonium, Thermochim. Acta 565 (2013) 151–158.
[4] S.M. Ennaceur, Study of the $\gamma \rightarrow \delta$ phase transformation kinetics and reaction mechanism in plutonium, Thermochim. Acta 566 (2013) 181–185.
[5] T.E. Mitchell, J.P. Hirth, D.S. Schwartz, J.N. Mitchell, The $\beta \rightarrow \alpha$ phase transformation in plutonium, Acta Mater. 61 (2013) 2895–2908.
[6] S.S. Hecker, D.R. Harbur, T.G. Zocco, Phase stability and phase transformations in Pu–Ga alloys, Prog. Mater. Sci. 49 (2004) 429–485.
[7] L. Kaufman, M. Cohen, Thermodynamics and kinetics of martensitic transformations, Prog. Metal. Phys. (1958) 165–246.
[8] K.T. Moore, C.R. Krenn, M.A. Wall, A.J. Schwartz, Orientation relationship, habit plane, twin relationship, interfacial structure, and plastic deformation resulting from the $\delta \rightarrow \alpha'$ isothermal martensitic transformation in Pu-Ga alloys, Metall. Mater. Trans. 38A (2007) 212–222.
[9] A. Goldberg, R.L. Rose, J.C. Shyne, Effects of stress and plastic deformation on the transformation of the δ phase in a Pu-1 at% Ga alloy, J. Nucl. Mater. 55 (1975) 33–52.
[10] P.H. Adler, G.B. Olson, D.S. Margolies, Kinematics of the δ to α and α to δ martensitic transformation in plutonium alloys, Acta Metall. 34 (1986) 2053–2064.
[11] Y.M. Jin, Y.U. Wang, A.G. Khachaturyan, C.R. Krenn, A.J. Schwartz, Crystallography of the $\delta \rightarrow \alpha$ martensitic transformation in plutonium alloys, Metall. Mater. Trans. 36A (2005) 2031–2047.
[12] J.P. Hirth, J.N. Mitchell, D.S. Schwartz, T.E. Mitchell, On the fcc → monoclinic martensite transformation in a Pu–1.7 at.% Ga alloy, Acta Mater. 54 (2006) 1917–1925.
[13] J.T. Orme, M.E. Faiers, B.J. Ward, The kinetics of the δ to α transformation in plutonium rich Pu-Ga alloys, in: Plutonium 1976 and Other Actinides, North-Holland Publishing Company, 1976, pp. 761–773.
[14] M.E. Faiers, R.G. Loasby, B.J. Ward, J.T. Orme, B.R. Spicer, Transformation kinetics of the α-β and δ-α transitions in pure and alloyed plutonium, in: Plutonium 1965, London, Chapman and Hall, 1965, pp. 64–87.
[15] B. Oudot, K.J.M. Blobaum, M.A. Wall, A.J. Schwartz, Supporting evidence of double-C curve kinetics in the isothermal δ to α' phase transformation in a Pu–Ga alloy, J. Alloys Compd. 444–445 (2007) 230–235.
[16] P. Deloffre, J.L. Truffier, A. Falanga, Phase transformation in Pu–Ga alloys at low temperature and under pressure: limit stability of the δ phase, J. Alloys Compd. 271–273 (1998) 370–373.
[17] B. Sadigh, W.G. Wolfer, Gallium stabilization of δ–Pu: density-functional calculations, Phys. Rev. B 72 (2005) 205122.
[18] P.H. Adler, Thermodynamic equilibrium in the low-solute regions of Pu-group MIA metal binary systems, Metall. Trans. A 22 (1991) 2237–2246.
[19] P.E.A. Turchi, L. Kaufman, S. Zhou, Z.K. Liu, Thermostatics and kinetics of transformations in Pu-based alloys, J. Alloys Comp. 444–445 (2007) 28–35.
[20] G. Texier, B. Oudot, C. Platteau, B. Ravat, F. Delaunay, Phase transformation in δ Pu alloys at low temperature: *in situ* dilatometric study, Mater. Sci. Eng. 9 (2010) 012033.
[21] B. Ravat, C. Plateau, G. Texier, B. Oudot, F. Delaunay, Phase transformations in δ–Pu alloys at low temperature: an *in situ* microstructural characterisation using X-ray diffraction, J. Nucl. Mater. 393 (2009) 418–424.
[22] K.J.M. Blobaum, J.R. Jeffries, A.J. Schwartz, H. Cynn, W. Yang, W.J. Evans, *In situ* X-ray diffraction study of the δ to α' isothermal martensitic transformation kinetics in a Pu-Ga alloy, J. Nucl. Mater. 412 (2011) 327–333.
[23] B. Ravat, B. Oudot, A. Perron, F. Lalire, F. Delaunay, Phase transformations in PuGa 1 at.% alloy, study of whole reversion process following martensitic transformations, J. Alloys Compd. 580 (2013) 298–309.
[24] A. Perron, B. Ravat, B. Oudot, F. Lalire, K. Mouturat, F. Delaunay, Phase transformations in Pu–Ga alloy: synergy between simulations and experiments to elucidate direct and indirect reversion competition, Acta Mater. 61 (2013) 7109–7120.
[25] C. Thiebaut, N. Baclet, B. Ravat, P. Giraud, P. Julia, Effect of radiation on bulk swelling of plutonium alloys, J. Nucl. Mater. 361 (2007) 184–191.
[26] B. Ravat, B. Oudot, N. Baclet, Study by XRD of the lattice swelling of PuGa alloys induced by self-irradiation, J. Nucl. Mater. 366 (2007) 288–296.
[27] J.R. Jeffries, K.J.M. Blobaum, M.A. Wall, A.J. Schwartz, Evidence for nascent equilibrium nuclei as progenitors of anomalous transformation kinetics in a Pu-Ga alloy, Phys. Rev. B 80 (2009) 094107.
[28] J.R. Jeffries, K.J.M. Blobaum, M.A. Wall, A.J. Schwartz, Microstructural evidence for conditioning-dependent δ to α' transformations in retained δ-phase Pu–Ga, Acta Mater. 57 (2009) 1831–1842.
[29] K.J.M. Blobaum, C.R. Krenn, M.A. Wall, T.B. Massalski, A.J. Schwartz, Nucleation and growth of the α martensitic phase in PuGa alloys, Acta Mater. 54 (2006) 4001–4011.
[30] J. Rodriguez-Carvajal, M.T. Fernandez-Diaz, J.L. Martinez, Neutron diffraction study on structural and magnetic properties of La_2NiO_4, J. Phys. Condens. Matter. 3 (1991) 3215–3234.
[31] W.H. Zachariasen, F.H. Ellinger, The crystal structure of alpha plutonium metal, Acta Cryst. 16 (1963) 777–783.
[32] F.H. Ellinger, Crystal structure of delta-prime plutonium and the thermal expansion characteristics of delta, delta-prime, and epsilon plutonium, J. Met. (1956) 1256–1259.
[33] C. Platteau, B. Ravat, G. Texier, B. Oudot, F. Delaunay, Microstructural analysis of the δ to α' phase transformation in plutonium alloys using X-ray diffraction, Mater. Sci. Eng. 9 (2010) 012092.
[34] A.C. Lawson, J.A. Roberts, B. Martinez, R.B. Von Dreele, B. Storey, H.T. Hawkins, M. Ramos, F.G. Hampel, C.C. Davis, R.A. Pereyra, J.N. Mitchell, F. Freibert, S.M. Valone, T.N. Claytor, D.A. Viskoe, F.W. Shonfeld, Lattice constants and anisotropic microstrain at low temperature in 242Pu-Ga alloys, Philos. Mag. B 85 (18) (2005) 2007–2022.
[35] V. Raghavan, A.R. Entwisle, The physical properties of martensite and bainite, special report n°93, Iron Steel Inst. (1965) 30.
[36] S.R. Pati, M. Cohen, Kinetics of isothermal martensitic transformations in an iron-nickel-manganese alloy, Acta Metall. 19 (1971) 1327–1332.
[37] J. Wong, M. Krisch, D.L. Farber, F. Occelli, R. Xu, T.-C. Chiang, D. Clatterbuck, A.J. Schwartz, M. Wall, C. Boro, Crystal dynamics of δ fcc Pu-Ga by high resolution inelastic X-ray scattering, Phys. Rev. B 72 (2005) 064115.
[38] C. Platteau, P. Bruckel, B. Ravat, F. Delaunay, PDF analysis of PuAl alloys local structure, J. Nucl. Mater. 385 (2009) 108–111.
[39] C.H. Shih, B.L. Averbach, M. Cohen, Some characteristics oft he isothermal martensitic transformation, Trans. Am. Inst. Min. Metall. Eng. 203 (1955) 183–187.
[40] J.R. Patel, M. Cohen, Criterion for the action of applied stress in the martensitic transformation, Acta Metall. 1 (1953) 531–538.
[41] P.H. Adler, G.B. Olson, M.F. Stevens, G.F. Gallegos, On the constitutive relations for the δ to α and α to δ martensitic transformation plasticity in plutonium alloys, Acta Metall. Mater. 40 (1992) 1073–1082.
[42] S.S. Hecker, Plutonium: coping with instability, J. Met. 55 (9) (2003) 13–19.
[43] R.L. Patterson, G.M. Wayman, The crystallography and growth of partially-twinned martensite plates in Fe-Ni alloys, Acta Metall. 14 (1966) 347–369.
[44] G. Miyamoto, A. Shibata, T. Maki, T. Furuhara, Precise measurement of strain accommodation in austenite matrix surrounding martensite in ferrous alloys by electron backscatter diffraction analysis, Acta Mater. 57 (2009) 1120–1131.
[45] X.M. Zhang, D.F. Li, Z.S. Xing, E. Gautier, J.S. Zhang, A. Simon, Morphology transition of deformation-induced lenticular martensite in Fe Ni C alloys, Acta Metall. Mater. 41 (1993) 1693–1699.
[46] X.M. Zhang, E. Gautier, A. Simon, Martensite morphology and habit plane transitions during tensile tests for Fe Ni C alloys, Acta Metall. 37 (1989) 477–485.
[47] T.J. Su, E. Aeby-Gautier, S. Denis, Morphology changes in bainite formed under stress, Scr. Mater. 54 (2006) 2185–2189.